

Reinforcing the no-lose theorem for NMSSM Higgs discovery at the LHC

M. M. Almarashi and S. Moretti

*School of Physics & Astronomy,
University of Southampton, Southampton, SO17 1BJ, UK*

Abstract

We show the potential of the LHC to detect a CP-even Higgs boson of the NMSSM, h_1 or h_2 , decaying into two rather light CP-odd Higgs bosons, a_1 , by exploiting the production mode based on Higgs-strahlung off b -quarks, i.e., the channel $pp \rightarrow b\bar{b}h_{1,2}$. We also consider the case of $h_2 \rightarrow h_1h_1$ decays. It is found that these decays have dominant BRs over large regions of the NMSSM parameter space where $\tan\beta$ is large, a condition which also favours the $pp \rightarrow b\bar{b}h_{1,2}$ production rates. Further decays of the light Higgs boson pairs (a_1 and h_1) into photon, muon, tau and b final states are also considered. The overall production and decay rates for these processes at inclusive level are sizable and should help extracting at least one Higgs boson signal over the NMSSM parameter space.

1 Introduction

The mechanism responsible for Electro-Weak Symmetry Breaking (EWSB) is still unknown. In the Standard Model (SM) and its extensions based on Supersymmetry (SUSY), such as the Minimal Supersymmetric Standard Model (MSSM) and the Next-to-Minimal Supersymmetric Standard Model (NMSSM), the Higgs mechanism is introduced for this primary purpose. Such a mechanism predicts the existence of at least one physical Higgs boson, which is a spin zero particle emerging from EWSB. While only one Higgs boson exists in the SM and five Higgs bosons in the MSSM, there are seven Higgs bosons in the NMSSM: three CP-even Higgses $h_{1,2,3}$ ($m_{h_1} < m_{h_2} < m_{h_3}$), two CP-odd Higgses $a_{1,2}$ ($m_{a_1} < m_{a_2}$) and two charged Higgses [1]. So, the latter has a phenomenologically richer Higgs sector than the two former scenarios.

The NMSSM has two additional merits over the MSSM. On the one hand, it can solve the so-called μ -problem of the MSSM [2] in a natural way by introducing a new gauge singlet

field [3]. On the other hand, it can relieve the little hierarchy problem [4, 5] since a SM-like scalar Higgs boson with mass less than the SM-like Higgs mass LEP limit is still quite naturally possible over some regions of the NMSSM parameter space. In fact, currently, the NMSSM can also explain a possible LEP excess and is definitely preferred by EW global fits. This happens when a SM-like Higgs boson of the NMSSM can unconventionally decay into two a_1 's with $m_{a_1} < 2m_b$ [6] (yet notice that this mass region is highly constrained by ALEPH [7] and BaBar [8] data). In fact, there is also another possibility in the NMSSM, due to the fact that $\text{BR}(a_1 \rightarrow \gamma\gamma)$ can be dominant and, as a result, $\text{BR}(a_1 \rightarrow b\bar{b})$ is suppressed even though $m_{a_1} > 2m_b$ [9, 10]. Finally, a CP-even Higgs state (h_1 or h_2) can naturally have a reduced couplings to the Z boson due to the mixing between the singlet and doublet Higgs fields, making it a natural possibility that the CP-even Higgs state of the NMSSM could have a mass less than the LEP limit on a SM-like Higgs mass.

Probing the Higgs sector of the NMSSM is experimentally challenging, as it is not certain that we can always detect its physical states. There has been some work dedicated to explore the detectability of at least one Higgs boson of the NMSSM at the Large Hadron Collider (LHC)¹ and the Tevatron. In particular, some efforts have been made to extend the so-called ‘no-lose theorem’ of the MSSM – stating that at least one Higgs boson of the MSSM will be discovered at the LHC via the usual SM-like production and decay channels throughout the entire MSSM parameter space [11] – to the case of the NMSSM [9, 10, 12, 13, 14, 15, 16]. By assuming that Higgs-to-Higgs decays are kinematically not allowed, it was realised that at least one Higgs boson of the NMSSM will be discovered at the LHC. However, this theorem could be violated if Higgs-to-Higgs and/or Higgs-to-SUSY particle (e.g., into neutralino pairs, yielding invisible Higgs signals) decays are kinematically accessible [17, 18].

So far, there is no conclusive evidence that the no-lose theorem can be confirmed in the context of the NMSSM. In order to establish the theorem for this SUSY scenario, Higgs-to-Higgs decays should definitely be taken into account though, in particular $h_1 \rightarrow a_1 a_1$. Such a decay can in fact be dominant in large regions of the NMSSM parameter space, for instance, for small A_k [9], and may not give Higgs signals with sufficient significance at the LHC. The importance of Higgs-to-Higgs decays in the context of the NMSSM has been emphasised over the years in much literature in all above respects, see, e.g., Refs. [5, 19, 20, 21]. Eventually, it was realised that Vector Boson Fusion (VBF)² could be a viable production channel to detect $h_{1,2} \rightarrow a_1 a_1$ at the LHC, in which the Higgs pair decays into $jj\tau^+\tau^-$ [12, 13, 22]. Some scope could also be afforded by a 4τ signature in both VBF and Higgs-strahlung (off gauge bosons) [23]. The gluon-fusion channel too could be a means of accessing $h_1 \rightarrow a_1 a_1$ decays, so long that the light CP-odd Higgs states both decay into four muons [24] or two muons and two taus [25]. Such results were all supported by simulations based on parton shower Monte Carlo (MC) programs and some level of detector response.

In this paper, we want to investigate whether or not the no-lose theorem of the NMSSM at the LHC can possibly be reinforced by considering a Higgs production channel so far neglected, i.e., Higgs boson production in association with b -quark pairs (aka Higgs-strahlung off b -quark pairs). Notice that the twin process in which b -quarks are replaced by t -quarks

¹Hereafter, we consider 14 TeV as LHC energy.

²Which is dominated by W^+W^- -fusion over ZZ -one.

was discussed in [15], where it was found to be very subleading over the NMSSM parameter space. We will be looking at inclusive event rates in presence of various Higgs-to-Higgs decays, $h_{1,2} \rightarrow a_1 a_1$ and $h_2 \rightarrow h_1 h_1$, for h_1 and h_2 produced in association with b -quark pairs. Notice that this production mode is in general the largest one in the NMSSM at large values of $\tan\beta$. We will also be studying the decay patterns of the lightest Higgs boson pairs, $a_1 a_1$ or $h_1 h_1$, into different types of decay modes.

This paper is organised as follows. In Sec. 2, we describe the parameter space scan performed. Inclusive event rates for the signals are explained in Sec. 3. Sec. 4 discusses possible signatures. Finally, we summarise and conclude in Sec. 5.

2 Parameter Space Scan

Due to the large number of parameters in the NMSSM, it is practically not feasible to do a comprehensive scan over all of them. Their number can however be reduced significantly by assuming certain conditions of unification. Since the mechanism of SUSY breaking is still unknown, to explore the NMSSM Higgs sector, we have performed a general scan in parameter space by fixing the soft SUSY breaking terms at high scale to reduce their contributions to the outputs of the parameter scans. Consequently, we are left with six independent inputs. Our parameter space is in particular defined through the Yukawa couplings λ and κ , the soft trilinear terms A_λ and A_κ plus $\tan\beta$ (the ratio of the Vacuum Expectation Values (VEVs) of the two Higgs doublets) and $\mu_{\text{eff}} = \lambda \langle S \rangle$ (where $\langle S \rangle$ is the vacuum expectation value of the Higgs singlet).

We used here the fortran package NMSSMTools developed in Refs. [26, 27]. This package computes the masses, couplings and decay widths of all the Higgs bosons of the NMSSM, including radiative corrections, in terms of its parameters at the EW scale. NMSSMTools also takes into account theoretical as well as experimental constraints from negative Higgs searches at LEP [28] and the Tevatron as well as other contexts (B -physics, low energy experiments, etc.), including the unconventional channels relevant for the NMSSM.

We have used the NMHDECAY code to scan over the six tree level parameters of the NMSSM Higgs sector in the following intervals:

$$\begin{aligned} \lambda : 0.0001 - 0.7, \quad \kappa : 0 - 0.65, \quad \tan\beta : 1.6 - 54, \\ \mu : 100 - 1000 \text{ GeV}, \quad A_\lambda : -1000 - +1000 \text{ GeV}, \quad A_\kappa : -10 - 0. \end{aligned}$$

Remaining soft terms, contributing at higher order level, which are fixed in the scan include:

- $m_{Q_3} = m_{U_3} = m_{D_3} = m_{L_3} = m_{E_3} = 1 \text{ TeV}$,
- $A_{U_3} = A_{D_3} = A_{E_3} = 1.2 \text{ TeV}$,
- $m_Q = m_U = m_D = m_L = m_E = 1 \text{ TeV}$,
- $M_1 = M_2 = M_3 = 1.5 \text{ TeV}$.

Notice that the sfermion mass parameters and the $SU(2)$ gaugino mass parameter, M_2 , play crucial roles in constraining $\tan\beta$. Decreasing values of those parameters allow smaller values of $\tan\beta$ to pass experimental and theoretical constraints. In fact, when $\tan\beta$ is large the sfermion masses should be large to avoid the constraints coming from the muon anomalous

magnetic moment [29]. The dominant supersymmetric contribution at large $\tan\beta$ is due to chargino-sneutrino loop diagram [30]. Also, notice that the chargino masses depend strongly on M_2 . As mentioned above, we fixed the gaugino mass parameters and other SUSY breaking terms at high scale to reduce their contributions to the outputs of the parameter scans.

In line with the assumptions made in [12, 13, 14], the allowed decay modes for neutral NMSSM Higgs bosons are³:

$$\begin{aligned} h, a \rightarrow gg, \quad h, a \rightarrow \mu^+\mu^-, \quad h, a \rightarrow \tau^+\tau^-, \quad h, a \rightarrow b\bar{b}, \quad h, a \rightarrow t\bar{t}, \\ h, a \rightarrow s\bar{s}, \quad h, a \rightarrow c\bar{c}, \quad h \rightarrow W^+W^-, \quad h \rightarrow ZZ, \\ h, a \rightarrow \gamma\gamma, \quad h, a \rightarrow Z\gamma, \quad h, a \rightarrow \text{Higgses}, \quad h, a \rightarrow \text{sparticles}. \end{aligned}$$

We have performed a random scan over 20 million points in the specified parameter space and required that $m_{h_2} \leq 300$ GeV. The output of the scan, as stated earlier, contains masses, Branching Ratios (BRs) and couplings of the NMSSM Higgses, for all the successful points, which have passed the various experimental and theoretical constraints.

3 Inclusive Event Rates

For successful data points, we used CalcHEP [31] to determine the cross-sections for NMSSM Higgs production⁴. As the SUSY mass scales have been arbitrarily set well above the EW one (see above), the NMSSM Higgs production modes exploitable in simulations at the LHC are those involving couplings to heavy ordinary matter only. Amongst the production channels onset by the latter, we focus here on the processes

$$gg, q\bar{q} \rightarrow b\bar{b} h_1 \quad \text{and} \quad gg, q\bar{q} \rightarrow b\bar{b} h_2, \quad (1)$$

i.e., Higgs production in association with a b -quark pair. This production mode is dominant at large $\tan\beta$.

To a good approximation, at large $\tan\beta$, the tree level lightest neutral Higgs boson masses are given by the following expressions [33]:

$$\begin{aligned} m_{a_1}^2 &= -\frac{3\kappa\mu_{\text{eff}}A_\kappa}{\lambda}, \\ m_{h_{1/2}}^2 &= \frac{1}{2} \left\{ m_Z^2 + \frac{\kappa\mu_{\text{eff}}}{\lambda} \left(\frac{4\kappa\mu_{\text{eff}}}{\lambda} + A_\kappa \right) \right. \\ &\quad \left. \mp \sqrt{\left[m_Z^2 - \frac{\kappa\mu_{\text{eff}}}{\lambda} \left(\frac{4\kappa\mu_{\text{eff}}}{\lambda} + A_\kappa \right) \right]^2 + \frac{\lambda^2 v^2}{2\mu_{\text{eff}}^2} \left[4\mu_{\text{eff}}^2 - m_A^2 \sin^2 2\beta \right]^2} \right\}, \end{aligned}$$

³Here, we use the label $h(a)$ to signify any of the neutral CP-even(odd) Higgs bosons of the NMSSM.

⁴We adopt herein CTEQ6L [32] as parton distribution functions, with scale $Q = \sqrt{\hat{s}}$, the centre-of-mass energy at parton level, for all processes computed. Further, we have taken $m_b(m_b) = 4.214$ GeV for the (running) bottom-quark mass.

where

$$m_A^2 = \frac{2\mu_{\text{eff}}}{\sin 2\beta} \left(A_\lambda + \frac{\kappa\mu_{\text{eff}}}{\lambda} \right).$$

(We reproduced here these tree level formulae mainly for guidance in interpreting the upcoming figures, the reader should recall though that NMSSMTools includes radiative corrections as well.)

To probe the NMSSM parameter space, we have computed m_{h_1} and m_{h_2} against each of the six parameters of the NMSSM (Figs. 1 and 2). As it is clear from the two figures, in our chosen parameter space regions, small values of λ , κ and μ_{eff} are favoured whereas large values of $\tan\beta$ and positive values of A_λ are the most compatible with theoretical and experimental data. The distribution over A_κ is uniform primarily because only small negative values of κ are scanned over.

Fig. 3 shows the correlations between all three Higgs masses, m_{a_1} , m_{h_1} and m_{h_2} . Since the successful points emerging from the scan have small values of λ , κ and also A_κ , only rather small values of m_{a_1} are allowed. It is remarkable that the smaller m_{a_1} the smaller m_{h_1} and m_{h_2} (two top-panes). In the bottom-pane of the same figure, for m_{h_2} around 120 GeV, m_{h_1} can have values from just above 0 up to slightly less than 120 GeV, showing the possibility that the two Higgs states can simultaneously have the same mass, $m_{h_1} \sim m_{h_2}$. Notice also that the majority of points have m_{h_1} between 115 GeV and 120 GeV, i.e., just above the LEP limit on a SM-like Higgs mass.

The production times decay rates of h_1 and h_2 , in which h_1 decays into two lighter a_1 's and h_2 decays into either a pair of a_1 's or a pair of h_1 's, as functions of the Higgs masses m_{h_1} and m_{h_2} (left-panes), $\tan\beta$ (middle-panes) and of the corresponding Higgs-to-Higgs decays BRs (right-panes), are shown in Fig.4. In our choice of parameter space which has large $\tan\beta$ we have noticed that the production rate of h_1 in association with a bottom-antibottom, $\sigma(pp \rightarrow b\bar{b}h_1)$, is nearly constant, does not depend on the tree level parameters, while the production rate of h_2 , $\sigma(pp \rightarrow b\bar{b}h_2)$, is strongly dependent on $\tan\beta$ and other tree level parameters. In fact, notice that in the figure we multiply the production rates by the decay rates of Higgs-to-Higgs particles, which play crucial roles in the changes of the inclusive cross section. The two bottom middle-panes of the figure make clear that while large $\tan\beta$ values are a necessary condition for large production times decay rates of h_2 they are not a sufficient one, as most of the points accumulate at intermediate event rates.

It is clear that Higgs-to-Higgs decays are dominant over a large area of NMSSM parameter space if Higgs-to-Higgs decays are kinematically allowed and so these decays should be taken seriously before claiming any validity (or otherwise) of the no-lose theorem for the NMSSM, see right-panes of Fig. 4. Fortunately, for considerable regions of parameter space, with different masses of h_1 and h_2 , these production rates are sizable (up to 1000 fb or so), except for the case of $h_2 \rightarrow h_1 h_1$ where only few points have large production rates, due to smallness of $\text{BR}(h_2 \rightarrow h_1 h_1)$ compared with $\text{BR}(h_{1,2} \rightarrow a_1 a_1)$ in general.

Fig. 5 displays the correlations between the three discussed production and decay processes. It is quite remarkable that the overall trend, despite an obvious spread also in the horizontal and vertical directions, is such that when one channel grows in event yield there is also another one which also does, hence opening up the possibility of the simultaneous

discovery of several Higgs states of the NMSSM (other than a_1 also h_1 and h_2), an exciting prospect in order to distinguish the NMSSM Higgs sector from the MSSM one.

In Fig. 6 we have calculated the signal rates of h_1 and h_2 through their cascade decays that finish with $a_1 \rightarrow b\bar{b}$ and/or $a_1 \rightarrow \tau^+\tau^-$. It is shown that the signal rates are quite large, topping 1000 fb for h_1 and 100 fb for h_2 in case of $4b$ and 4τ final states due to the fact that $\text{BR}(a_1 \rightarrow b\bar{b})$ is dominant when $m_{a_1} \geq 10$ GeV and $\text{BR}(a_1 \rightarrow \tau^+\tau^-)$ is dominant for $m_{a_1} < 10$ GeV. The $2b$ plus 2τ rates are one order of magnitude less than the former two due to the fact that only the parameter space points with $m_{a_1} \geq 10$ GeV have these final states in which $\text{BR}(a_1 \rightarrow \tau^+\tau^-)$ is only about 10% of $\text{BR}(a_1 \rightarrow b\bar{b})$. Overall, there are some regions of parameter space which have considerable signal rates that could be sufficient to discover the h_1 and h_2 through their $a_1 a_1$ cascade decays at the LHC.

The h_2 cascade decays ending with $h_1 \rightarrow b\bar{b}$ and/or $h_1 \rightarrow \tau^+\tau^-$ have less cross section (see Fig. 7). Only for m_{h_2} around 120 GeV the rates are quite sizable, topping 50 fb, 5 fb and 0.5 fb level for $4b$, $2b$ plus 2τ and 4τ final states, respectively.

As explained in Ref. [9], the $\text{BR}(a_1 \rightarrow \gamma\gamma)$ can be dominant over a sizable region of NMSSM parameter space. This very peculiar phenomenon appears in this SUSY scenario (unlike the MSSM) because of the fact that a rather light CP-odd Higgs state can have a predominant singlet component and a very weak doublet one. As a consequence, all SM-like partial decay widths are heavily suppressed as they employ only the doublet component, except one: $\Gamma(a_1 \rightarrow \gamma\gamma)$. This comes from the fact that the $a_1 \rightarrow \tilde{\chi}^+ \tilde{\chi}^-$ coupling is not suppressed, as it is generated through the $\lambda H_1 H_2 S$ Lagrangian term and therefore implies no small mixing. Although the direct decay $a_1 \rightarrow \tilde{\chi}^+ \tilde{\chi}^-$ is forbidden, the aforementioned coupling participates in the $a_1 \gamma\gamma$ effective coupling. In hence, when $\text{BR}(a_1 \rightarrow \gamma\gamma)$ is very large, no other SM-like BR can be. Hence, it makes sense to look at the scope of $a_1 a_1 \rightarrow \gamma\gamma\gamma\gamma$ decays. The corresponding inclusive rates are found in Fig. 8 as functions of m_{h_1} and m_{h_2} (two top-panes) for both $h_1 \rightarrow a_1 a_1 \rightarrow 4\gamma$ and $h_2 \rightarrow a_1 a_1 \rightarrow 4\gamma$. Despite inclusive rates are never very large, it should be noticed a consistent population of points in the former case at $m_{h_1} \approx 115$ GeV yielding up to $\mathcal{O}(1)$ fb rates, with also a possibility of rates reaching up to 100 fb for smaller m_{h_1} , and in the latter case well spread out in m_{h_2} from 115 to 300 GeV yielding some points between 0.1 and 1 fb. Moreover, we have shown in the same figure the inclusive results for $h_1 \rightarrow a_1 a_1 \rightarrow \tau^+ \tau^- \mu^+ \mu^-$ and $h_2 \rightarrow a_1 a_1 \rightarrow \tau^+ \tau^- \mu^+ \mu^-$. The rates for h_1 can reach 1 fb^{-1} for various ranges of m_{h_1} and roughly 0.5 fb^{-1} in case of h_2 for essentially any m_{h_2} .

Finally, notice that the cases $h_1 \rightarrow a_1 a_1 \rightarrow \mu^+ \mu^- \mu^+ \mu^-$ and $h_2 \rightarrow a_1 a_1 \rightarrow \mu^+ \mu^- \mu^+ \mu^-$ contribute below the 0.01 fb level over the entire NMSSM parameter space, so we do not show the corresponding plots.

4 Possible Signatures

The production times decay rates presented in the previous section are inclusive results, whereby no cuts have been enforced on the final state particles⁵. Clearly, in order to detect

⁵Recall that we use a finite b -quark mass, see Footnote 4.

the latter, a typical finite volume of an LHC detector has to be emulated. Further, in order to assess the significance of the signal yield, a background simulation (within the same detector region) has to eventually be carried out. Here, in the spirit of Ref. [15], we would like to discuss the possible scope of the possible aforementioned signatures, without however venturing in such a complicated simulations. The key issue to be accessed is clearly whether one or more of the b -quarks produced in association with the Higgs state h_1 or h_2 (henceforth called ‘prompt’ b -quarks) in process (1) ought to be tagged as such. The relevance of this should be clear from inspecting Fig. 9. The b -quarks in the final state often emerges from the splitting of a gluon inside the proton, hence they can be at very low transverse momentum (denoted here by p_{T_b}). To enforce vertex tagging with good efficiency, say $\varepsilon_b = 60\%$, a minimum p_{T_b} value is always required, the lowest reasonable threshold being 15 GeV or so [34, 35]. For the case of a single b -tag the overall efficiency at very low Higgs masses (irrespective of considering either h_1 or h_2 being produced) is some 2–3%, eventually growing to 14–15% for very massive objects. For the case of a double b -tag, we are instead speaking of corresponding rates at the 1% to 8% level, respectively. Clearly then, the scope of the production and decay channels investigated in the previous section much depends on the Higgs mass produced and the decay patterns pursued.

We reckon that for the 4γ signature it should not be necessary to tag any of the ‘prompt’ b -quarks at all, as any of the (typically high transverse momentum and isolated) decay products of the a_1 ’s could act as trigger and the SM backgrounds (which would generally be induced by non-QCD processes) should not be prohibitively large⁶. Regarding signatures with τ ’s, for 4τ and $2\tau 2b$ one could certainly exploit a τ trigger (both leptonic and hadronic) [34, 35], however (especially in case of hadronic τ decays), it may be necessary to tag at least one ‘prompt’ b -quark to suppress QCD backgrounds mimicking $\tau \rightarrow$ hadrons. The case $2\tau 2\mu$ would clearly exploit a muon trigger instead. Finally, the case of a $4b$ signature of $h_{1,2} \rightarrow a_1 a_1$ and $h_2 \rightarrow h_1 h_1$ decays is totally unexplored, especially considering the fact that the entire final state would be made up of six quarks, i.e., with an unavoidable huge combinatorics and burdened by an extremely large pure QCD background.

In essence, only a dedicated kinematical analysis of the decay products could in the end ascertain the true selection efficiency of a signature and its scope. What we can responsibly do here is to highlight three possible scenarios. Firstly, one whereby the signal rates in the proceeding section will not be reduced substantially after enforcing acceptance cuts: this is certainly applicable to 4γ events emerging from a_1 states with masses between 50 and 100 GeV (where the $\text{BR}(a_1 \rightarrow \gamma\gamma)$ is maximal, see bottom-left pane of Fig. 2 in [9]) and 4τ events (with the heavy leptons decaying leptonically to electron and muons, which however induce a 1% suppression because of the consequent BRs). Secondly, one whereby all decay signatures involving (one or more) hadronic τ ’s and b ’s are reduced by a factor between 7 and 50, depending on the produced Higgs mass, assuming a single tag only of ‘prompt’ b ’s. Thirdly, one whereby most possibly the $6b$ final state requires a double tag of ‘prompt’ b -quarks, reducing the signal yield by a factor between 20 and 100, depending on the $h_{1,2}$

⁶This is in fact very important in view of the fact that the 4γ decay rate is the smallest one amongst those studied here.

mass⁷.

Conclusions

Searching for NMSSM Higgs states at the LHC is very complicated compared to the MSSM ones due to the dominance of Higgs-to-Higgs decays in large parameter space regions of the next-to-minimal SUSY model. This is the main reason why a no-lose theorem has not been confirmed yet in the context of the NMSSM. In view of this and following on previous work, where the case of VBF and Higgs-strahlung of W, Z bosons and t quarks was studied [15], we have found here that, at large values of $\tan\beta$, h_1 and h_2 production in association with bottom-antibottom pairs and decaying into lighter Higgses can have sizable signal rates in some regions of NMSSM parameter space, in a variety of decay patterns including photons, muons, taus and b -quarks themselves. We have verified this at the inclusive level and discussed what could happen in presence of acceptance cuts and consequent detector efficiencies.

Clearly, in the end, only a dedicated decay analysis, in presence of not only acceptance but also selection cuts (the latter driven by the also necessary background assessment), will decree whether signal extraction is possible and through which signatures. However, our present study, alongside the findings of [15], should eventually direct the NMSSM parameter space exploration where discovery significances can be found. In all circumstances, just like with other previous attempts at extracting NMSSM Higgs-to-Higgs signatures, evidence of those investigated here will require a rather large LHC luminosity sample, of $\mathcal{O}(100 \text{ fb}^{-1})$ or more.

Acknowledgments

This work is supported in part by the NExT Institute. M. M. A. acknowledges a scholarship granted to him by Taibah University (Saudi Arabia).

⁷Notice that for a_1 masses comparable to typical transverse momentum thresholds of the decay products further severe reductions could occur, however, there is plenty of NMSSM parameter space giving sizable signals for heavier a_1 states for all signatures considered here.

References

- [1] For reviews, see: e.g., U. Ellwanger, C. Hugonie and A. M. Teixeira, Phys. Rept. **496** (2010) 1 (and references therein); M. Maniatis, Int. J. Mod. Phys. A **25** (2010) 3505 (and references therein).
- [2] J. E. Kim and H. P. Nilles, Phys. Lett. B **138** (1984) 150.
- [3] J. R. Ellis, J. F. Gunion, H. E. Haber, L. Roszkowski and F. Zwirner, Phys. Rev. D **39** (1989) 844.
- [4] M. Bastero-Gil, C. Hugonie, S. F. King, D. P. Roy and S. Vempati, Phys. Lett. B **489** (2000) 359.
- [5] R. Dermisek and J. F. Gunion, Phys. Rev. Lett. **95** (2005) 041801.
- [6] R. Dermisek and J. F. Gunion, Phys. Rev. D **76** (2007) 095006.
- [7] S. Schael *et al.* [ALEPH Collaboration], JHEP **1005** (2010) 049.
- [8] B. Aubert *et al.* [BABAR Collaboration], Phys. Rev. Lett. **103** (2009) 181801.
- [9] M. Almarashi and S. Moretti, Eur. Phys. J. C **71** (2011) 1618.
- [10] M. Almarashi and S. Moretti, arXiv:1105.4191 [hep-ph].
- [11] J. Dai, J. F. Gunion and R. Vega, Phys. Lett. B **315** (1993) 355 and Phys. Lett. B **345** (1995) 29; J.R. Espinosa and J. F. Gunion, Phys. Rev. Lett. **82** (1999) 1084.
- [12] U. Ellwanger, J. F. Gunion and C. Hugonie, JHEP **0507** (2005) 041.
- [13] U. Ellwanger, J. F. Gunion, C. Hugonie and S. Moretti, arXiv:hep-ph/0305109.
- [14] U. Ellwanger, J.F. Gunion and C. Hugonie, hep-ph/0111179; D.J. Miller and S. Moretti, hep-ph/0403137; C. Hugonie and S. Moretti, hep-ph/0110241; A. Belyaev, S. Hesselbach, S. Lehti, S. Moretti, A. Nikitenko and C. H. Shepherd-Themistocleous, arXiv:0805.3505 [hep-ph]; J. R. Forshaw, J. F. Gunion, L. Hodgkinson, A. Papaefstathiou and A. D. Pilkington, JHEP **0804** (2008) 090; A. Belyaev, J. Pivarski, A. Safonov, S. Senkin and A. Tatarinov, Phys. Rev. D **81** (2010) 075021.
- [15] S. Moretti, S. Munir and P. Poulose, Phys. Lett. B **644** (2007) 241.
- [16] M. M. Almarashi and S. Moretti, Phys. Rev. D **83** (2011) 035023.
- [17] U. Ellwanger and C. Hugonie, Eur. Phys. J. C **25** (2002) 297.
- [18] A. Djouadi *et al.*, JHEP **0807** (2008) 002; F. Mahmoudi, J. Rathsmann, O. Stal and L. Zeune, Eur. Phys. J. C **71** (2011) 1608.

- [19] J. F. Gunion, H. E. Haber and T. Moroi, *In the Proceedings of 1996 DPF / DPB Summer Study on New Directions for High-Energy Physics (Snowmass 96), Snowmass, Colorado, 25 Jun - 12 Jul 1996, pp LTH095* [arXiv:hep-ph/9610337].
- [20] B. A. Dobrescu, G. L. Landsberg and K. T. Matchev, Phys. Rev. D **63** (2001) 075003.
- [21] B. A. Dobrescu and K. T. Matchev, JHEP **0009** (2000) 031.
- [22] U. Ellwanger, J. F. Gunion, C. Hugonie and S. Moretti, arXiv:hep-ph/0401228.
- [23] A. Belyaev, S. Hesselbach, S. Lehti, S. Moretti, A. Nikitenko and C. H. Shepherd-Themistocleous, in Ref. [14].
- [24] A. Belyaev, J. Pivarski, A. Safonov, S. Senkin and A. Tatarinov, in Ref. [14].
- [25] M. Lisanti and J.G. Wacker, Phys. Rev. D **79** (2009) 115006.
- [26] U. Ellwanger, J.F. Gunion and C. Hugonie, JHEP **0502** (2005) 066; U. Ellwanger and C. Hugonie, Comput. Phys. Commun. **175** (2006) 290.
- [27] See <http://www.th.u-psud.fr/NMHDECAY/nmssmtools.html>.
- [28] S. Schael *et al.*, Eur. Phys. J. C **47** (2006) 547.
- [29] F. Domingo and U. Ellwanger, JHEP **0807** (2008) 079
- [30] A. Czarnecki and W. J. Marciano, Phys. Rev. D **64** (2001) 013014.
- [31] A. Pukhov, arXiv:hep-ph/0412191.
- [32] See <http://hep.pa.msu.edu/cteq/public/cteq6.html>.
- [33] D.J. Miller, R. Nevzorov and P.M. Zerwas, Nucl. Phys. B **681** (2004) 3.
- [34] ATLAS Collaboration, arXiv:0901.0512 [hep-ex].
- [35] CMS Collaboration, J. Phys. G **34** (2007) 995.

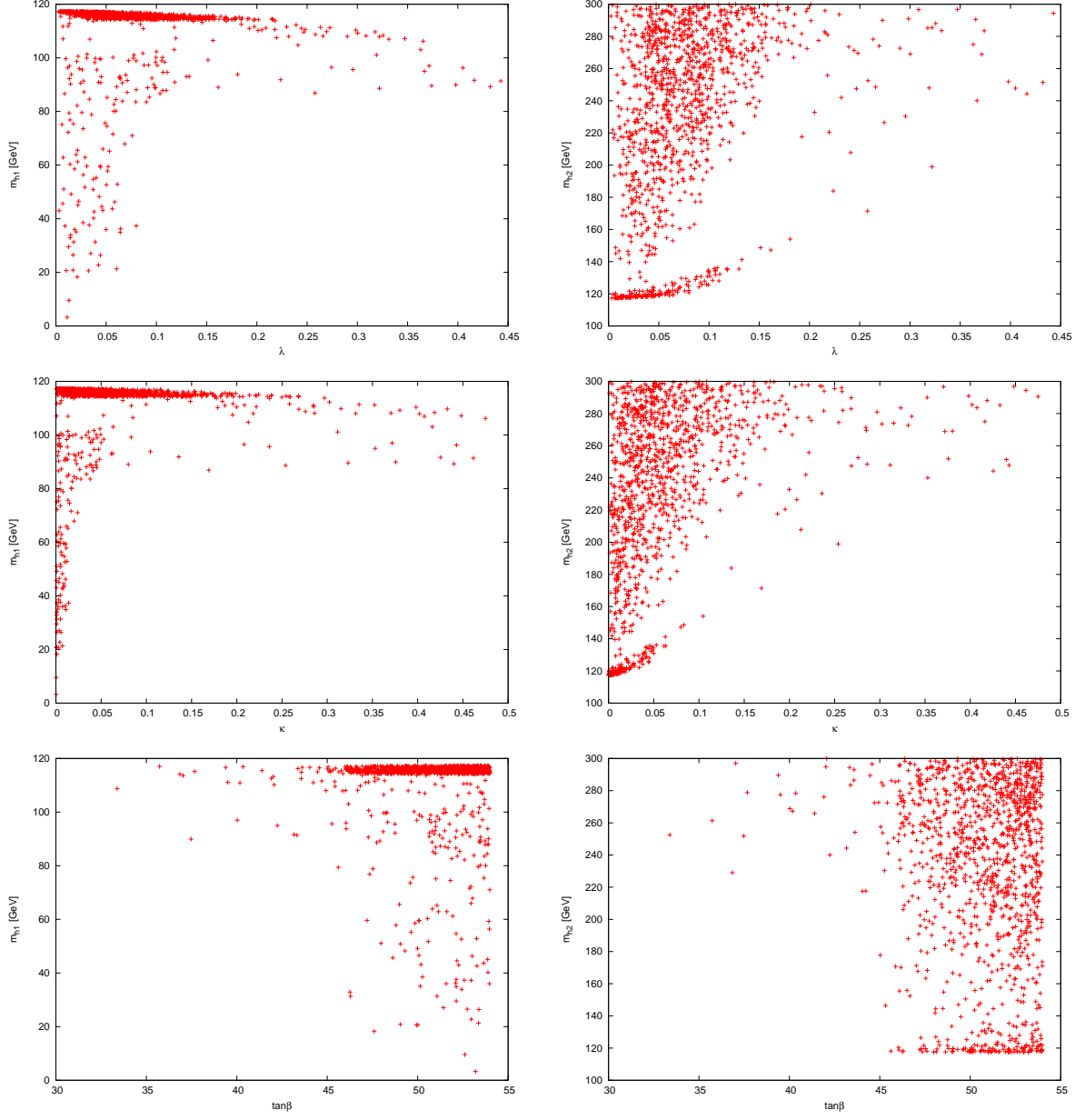


Figure 1: The lightest two scalar Higgs masses m_{h_1} and m_{h_2} as functions of λ , κ and $\tan\beta$.

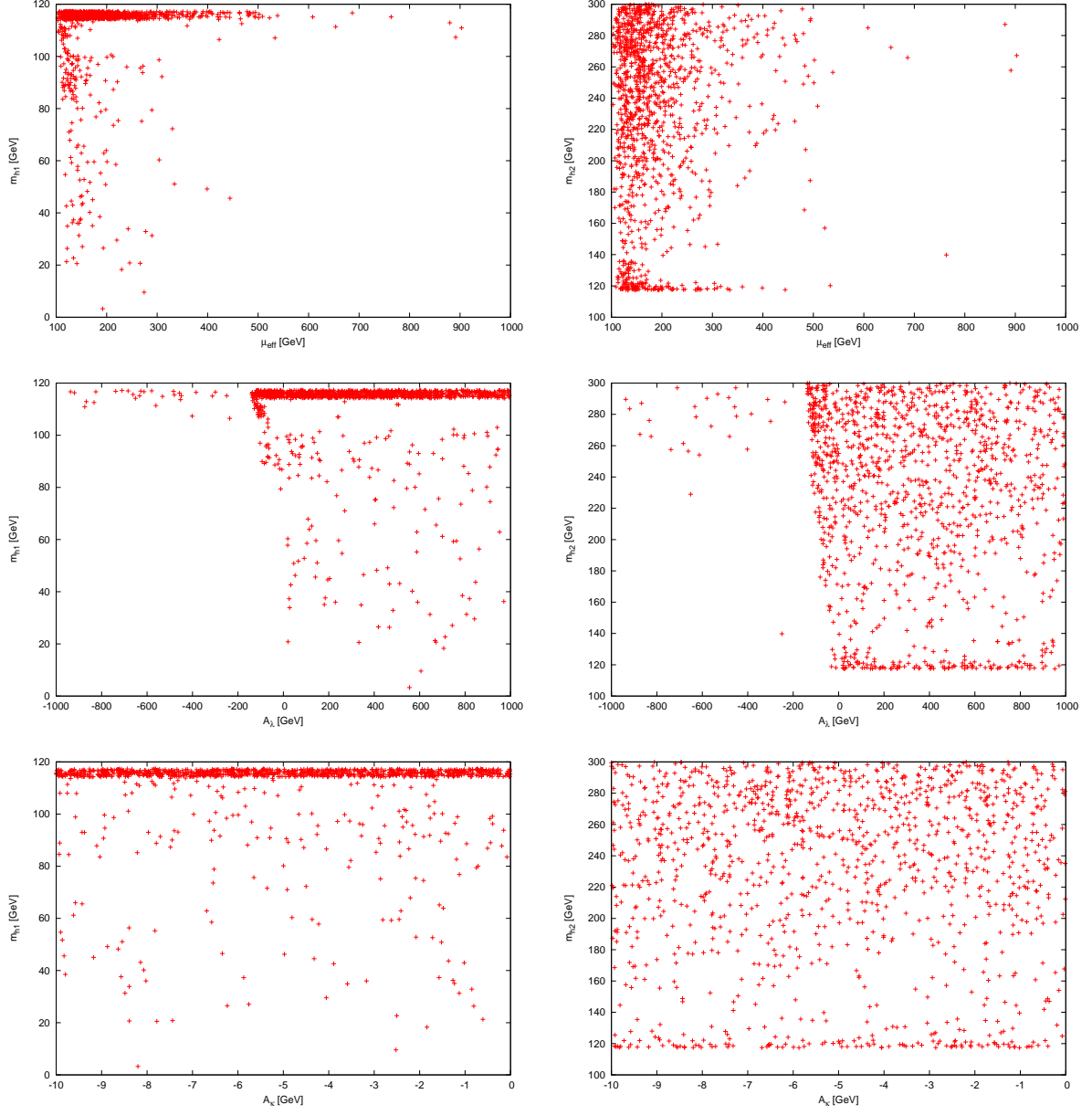


Figure 2: The lightest two scalar Higgs masses m_{h_1} and m_{h_2} as functions of μ_{eff} , A_λ and A_κ .

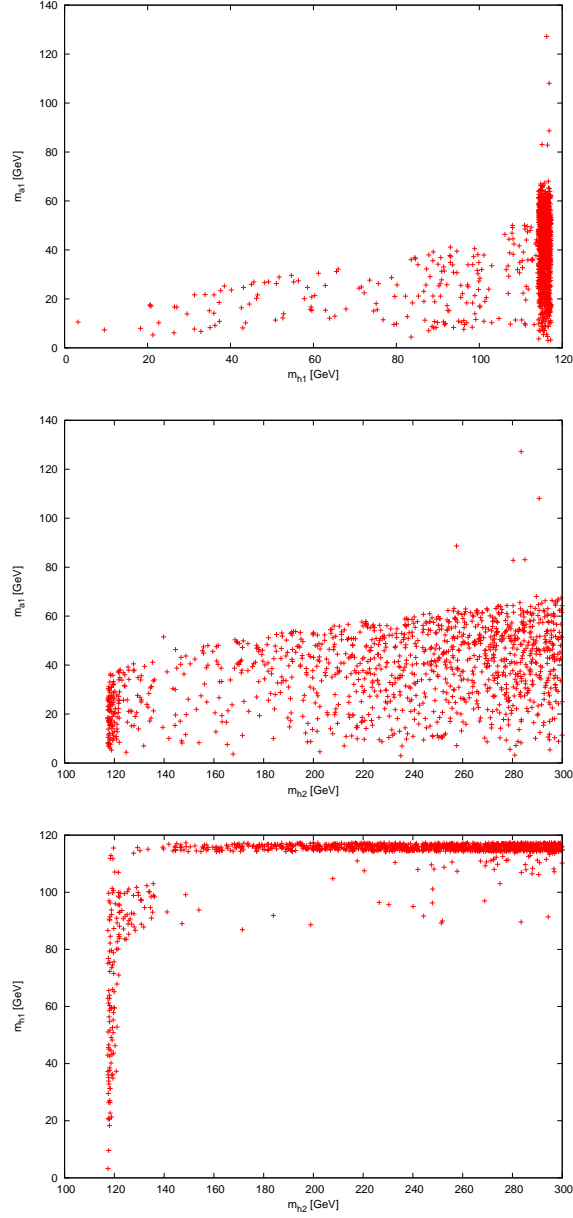


Figure 3: The correlations between the lightest CP-odd Higgs mass, m_{a_1} and the lightest two CP-even Higgs masses, m_{h_1} and m_{h_2} and between the latter two.

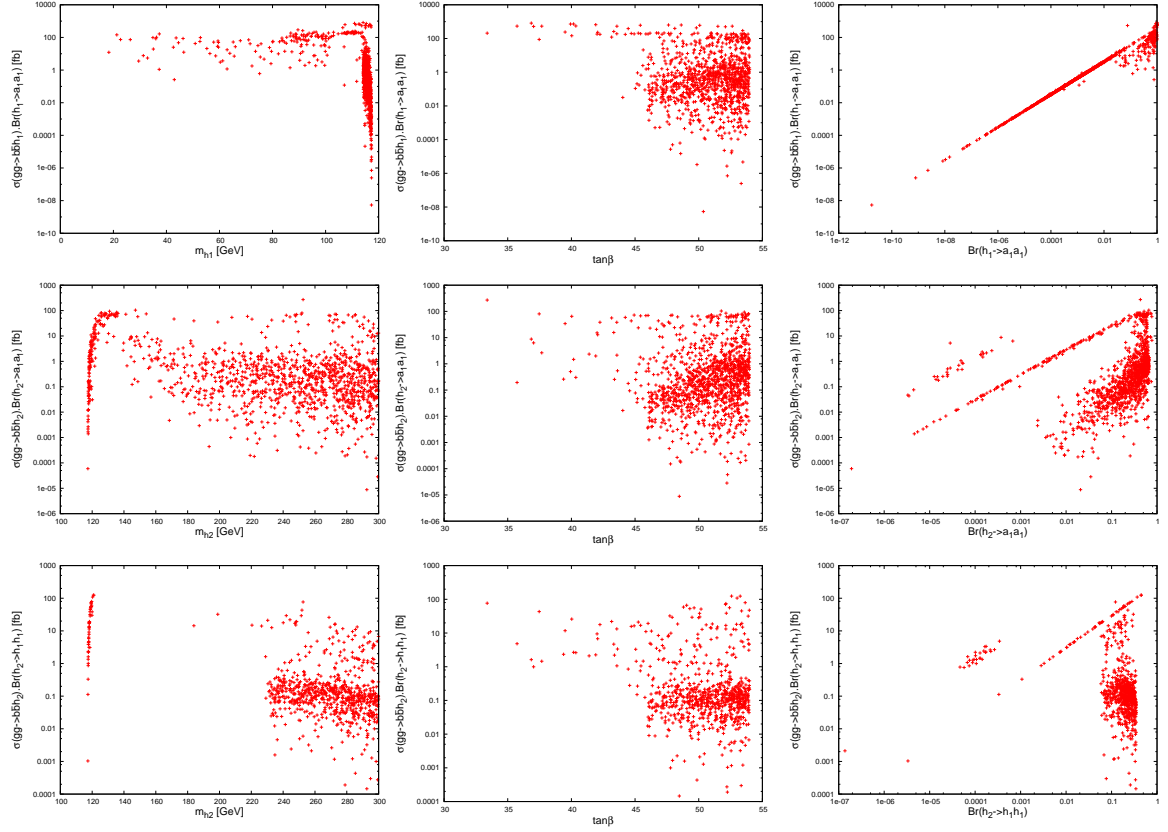


Figure 4: The rates for $\sigma(pp \rightarrow b\bar{b}h_1) \text{BR}(h_1 \rightarrow a_1a_1)$, $\sigma(pp \rightarrow b\bar{b}h_2) \text{BR}(h_2 \rightarrow a_1a_1)$ and $\sigma(pp \rightarrow b\bar{b}h_2) \text{BR}(h_2 \rightarrow h_1h_1)$ as functions of corresponding Higgs masses, of $\tan\beta$ and of corresponding BRs.

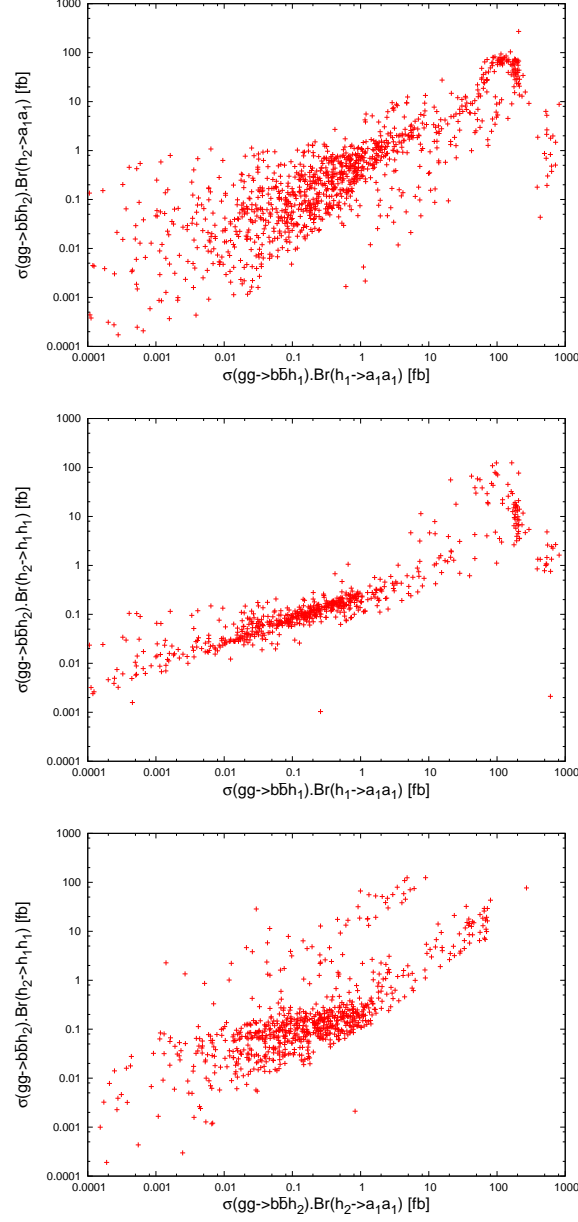


Figure 5: The rates for $\sigma(pp \rightarrow b\bar{b}h_1) \text{Br}(h_1 \rightarrow a_1 a_1)$ versus $\sigma(pp \rightarrow b\bar{b}h_2) \text{Br}(h_2 \rightarrow a_1 a_1)$, for $\sigma(pp \rightarrow b\bar{b}h_1) \text{Br}(h_1 \rightarrow a_1 a_1)$ versus $\sigma(pp \rightarrow b\bar{b}h_2) \text{Br}(h_2 \rightarrow h_1 h_1)$ and for $\sigma(pp \rightarrow b\bar{b}h_1) \text{Br}(h_2 \rightarrow a_1 a_1)$ versus $\sigma(pp \rightarrow b\bar{b}h_2) \text{Br}(h_2 \rightarrow h_1 h_1)$.

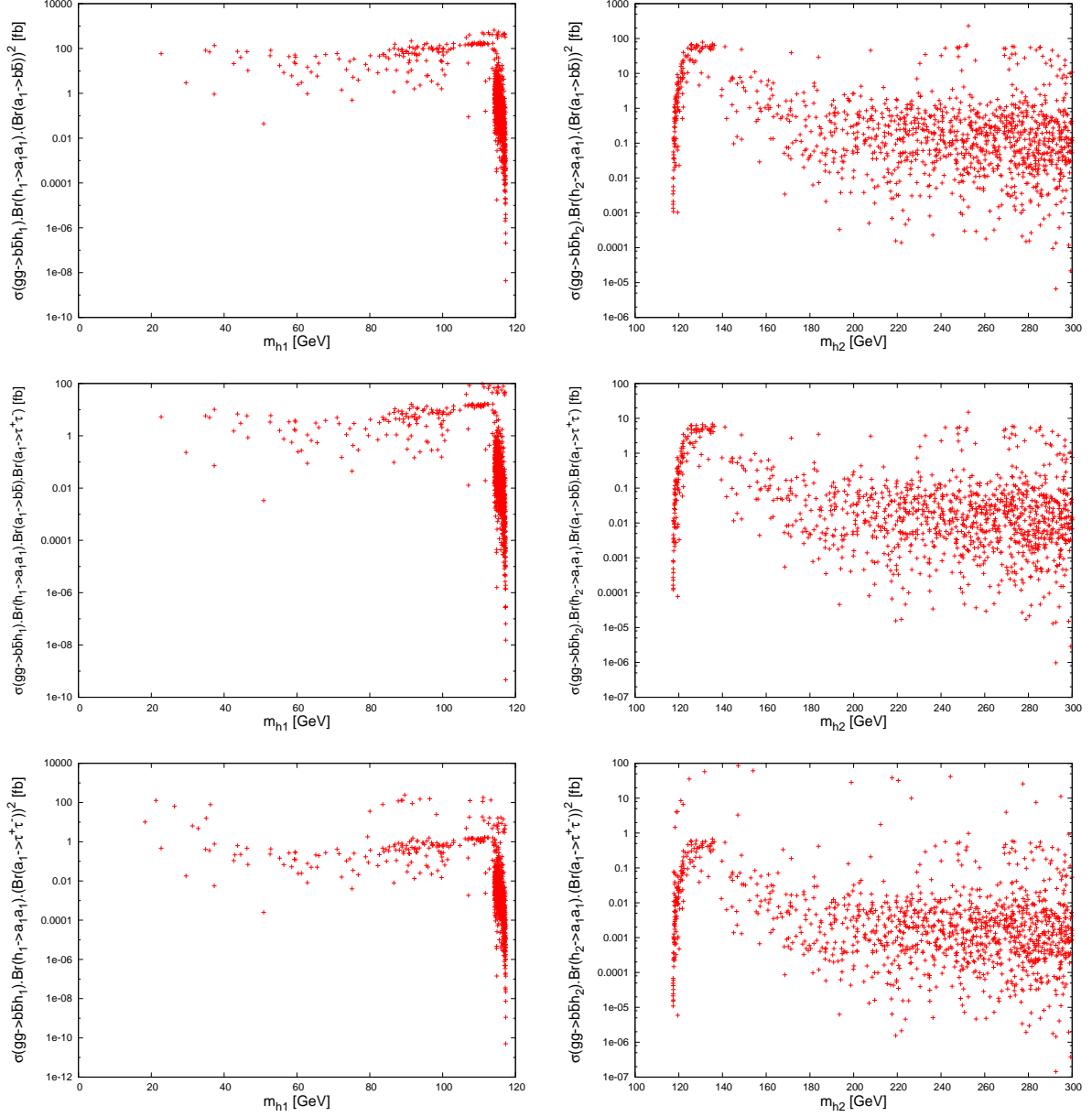


Figure 6: The signal rates for $\sigma(pp \rightarrow b\bar{b}h_1) \text{BR}(h_1 \rightarrow a_1 a_1)$ and $\sigma(pp \rightarrow b\bar{b}h_2) \text{BR}(h_2 \rightarrow a_1 a_1)$ times $\text{BR}(a_1 a_1 \rightarrow b\bar{b}b\bar{b})$, $\text{BR}(a_1 a_1 \rightarrow b\bar{b}\tau^+\tau^-)$ and $\text{BR}(a_1 a_1 \rightarrow \tau^+\tau^-\tau^+\tau^-)$ as functions of m_{h_1} and m_{h_2} .

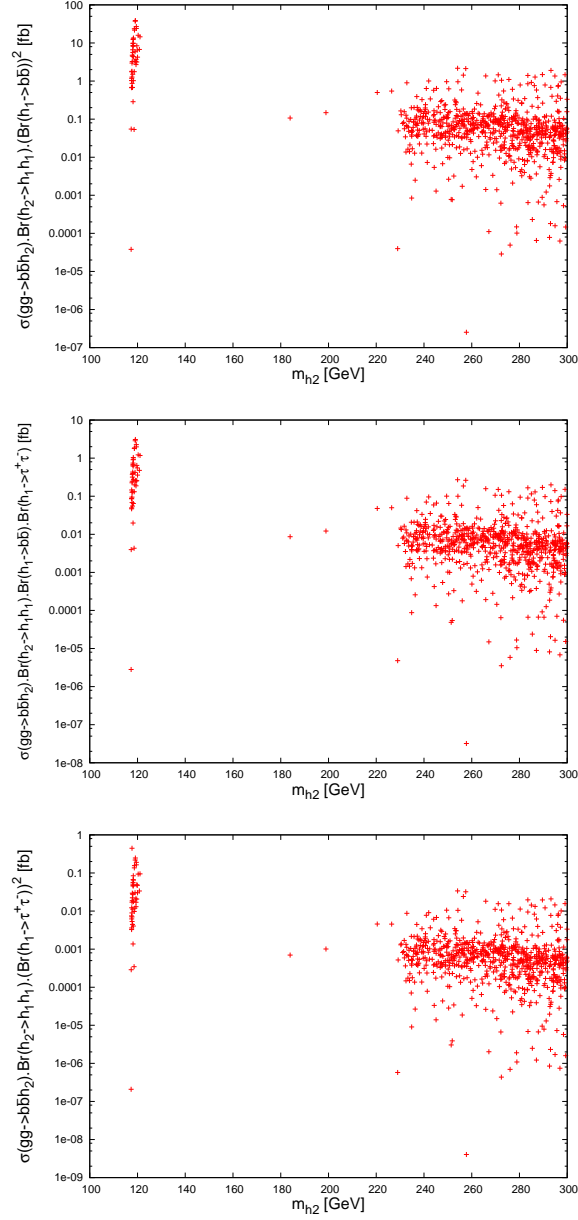


Figure 7: The signal rates for $\sigma(pp \rightarrow b\bar{b}h_2) \text{BR}(h_2 \rightarrow h_1 h_1)$ times $\text{BR}(h_1 h_1 \rightarrow b\bar{b}b\bar{b})$, $\text{BR}(h_1 h_1 \rightarrow b\bar{b}\tau^+\tau^-)$ and $\text{BR}(h_1 h_1 \rightarrow \tau^+\tau^-\tau^+\tau^-)$ as functions of m_{h_2} .

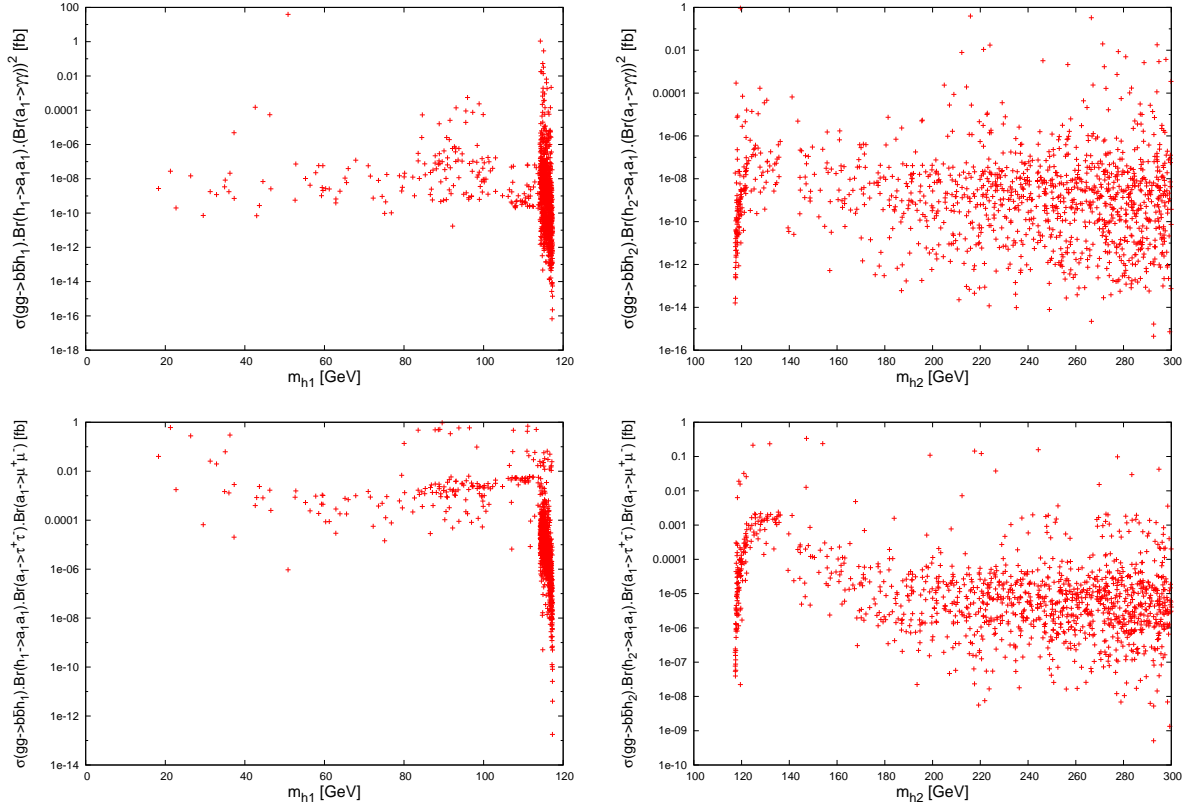


Figure 8: The signal rates for $\sigma(pp \rightarrow b\bar{b}h_1) \text{BR}(h_1 \rightarrow a_1 a_1)$ and $\sigma(pp \rightarrow b\bar{b}h_2) \text{BR}(h_2 \rightarrow a_1 a_1)$ times $(\text{BR}(a_1 \rightarrow \gamma\gamma))^2$ and times $\text{BR}(a_1 \rightarrow \tau^+\tau^-) \text{BR}(a_1 \rightarrow \mu^+\mu^-)$ as functions of m_{h_1} and m_{h_2} .

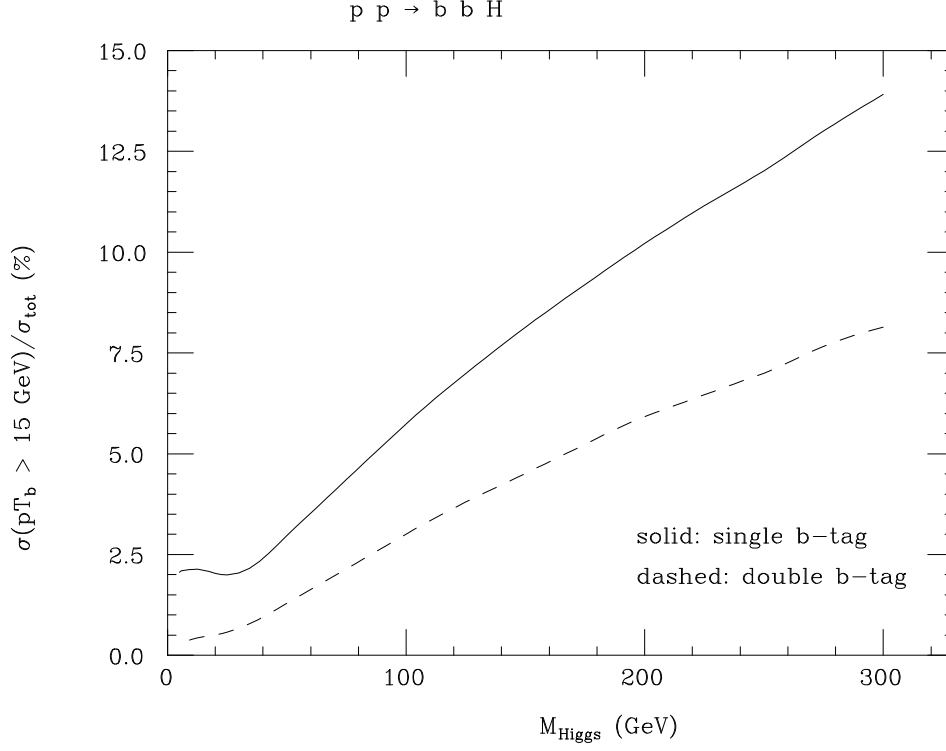


Figure 9: The efficiency to tag one or two ‘prompt’ b -quarks in the final state, given as percent ratio of the production cross section for $pp \rightarrow b\bar{b} \text{ Higgs}$ (where Higgs can equally refer to an h_1 or h_2 state) after a the cut $p_{T_b} > 15 \text{ GeV}$ over the total one (also including the b -tagging performances, ε_b and ε_b^2 , respectively), as function of the Higgs boson mass. The distributions have been produced at parton level by using CalcHEP. Herein we use $\varepsilon_b = 60\%$.